

**Brushless
Permanent Magnet
Motor Design**
Second Edition

Dr. Duane Hanselman

Electrical and Computer Engineering
University of Maine
Orono, ME 04469
USA
brushlessmotor@ieee.org
www.eece.maine.edu/motor

THE WRITERS' COLLECTIVE

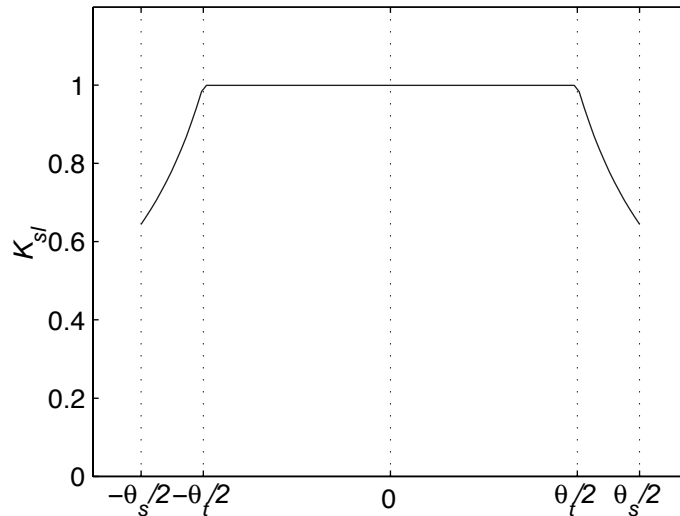


Figure 7-3. Typical slot correction factor.

density at the slot midpoint is reduced to about 65% of its nominal value by the slot correction factor. The depth of this notch is highly dependent on the width of the slot opening. In many typical cases, it is not as deep as that shown in Fig. 7-3.

This slot correction modeling assumes that the magnetic field is unchanged over the entire surface of the tooth. In reality, the magnetic field begins to experience some degradation as one approaches the slot area. As a result, some slot correction derivations extend their correction over the shoe tip area by an empirically-determined amount that is a function of the slot opening.

There is no consensus about the optimum way to determine the slot correction factor. Shoe tip saturation and the finite radial depth of the shoe make it difficult to predict the slot correction factor accurately using an analytic expression. Each approach has its strengths and weaknesses. In practice, the differences in tooth flux computed using different slot correction factors are not dramatically different because integration is a naturally smoothing process.

7.3 Tooth Flux

Because all coils in a motor can be described in terms of a sequence of equivalent single tooth coils as described in Chapter 6, the flux linked by each coil is the sum of that linked to the individual tooth coils. For example, consider the coil and its single tooth equivalent shown in Fig. 7-4. If $\phi_1(\theta)$ describes the flux in the first tooth as a

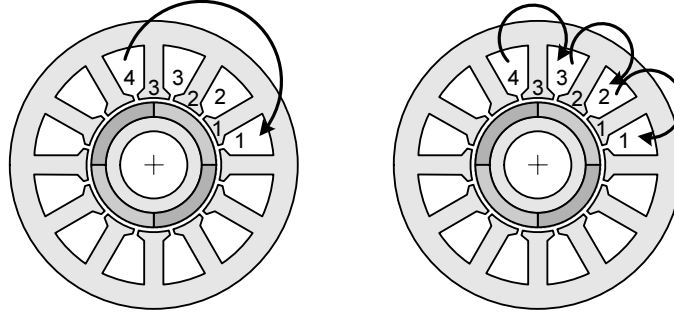


Figure 7-4. A coil and its single tooth equivalent.

function of the rotor position θ in electrical measure, then the flux in the second tooth is $\phi_2(\theta) = \phi_1(\theta - \theta_s)$ where θ_s is the angular tooth or slot offset in electrical measure. Similarly, $\phi_3(\theta) = \phi_1(\theta - 2\theta_s)$ is the flux in the third tooth making up the coil. Then the flux linking the coil on the left in the figure is $\phi_c(\theta) = \phi_1(\theta) + \phi_1(\theta - \theta_s) + \phi_1(\theta - 2\theta_s)$.

As described above, the tooth flux plays a crucial role in determining motor performance. From basic principles, this flux is given by the integral of the flux density over one slot pitch and axial motor length as

$$\phi = \int \vec{B} \cdot d\vec{A}$$

which, for the geometry shown in Fig. 7-5 becomes

$$\phi_t(\alpha) = \int_{-L_{st}/2}^{L_{st}/2} \int_{-\theta_s/2}^{\theta_s/2} K_{sl}(\theta) B_{gs}(\theta + \alpha) R_s d\theta dz \quad (7.12)$$

where L_{st} is the axial motor length, $B_{gs}(\theta)$ is given by (7.6), all angles are in mechanical measure, and α is the angular offset between a tooth center and magnet center. Since the integrand is not a function of the axial dimension z , the outer integral becomes multiplication by L_{st} . Furthermore, since the tooth flux is periodic with a period equal to the electrical period, (7.12) can be rewritten as

$$\phi_t(\alpha) = \frac{2L_{st}R_s}{N_m} \int_{-\theta_s/2}^{\theta_s/2} K_{sl}(\theta) B_{gs}(\theta + \alpha) d\theta \quad (7.13)$$

where all angles are now in electrical measure.

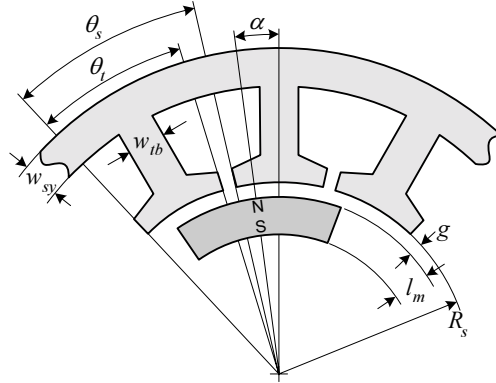


Figure 7-5. Geometry for computation of tooth flux.

For simplicity, let $B_{gs}(\theta)$ as given in (7.6) be written as the Fourier series in electrical measure as

$$B_{gs}(\theta) = \sum_{n=-\infty}^{\infty} B_{gn} e^{jn\theta} \tag{7.14}$$

Substituting this expression into (7.13) and simplifying produces the Fourier series description for the tooth flux of

$$\phi_t(\alpha) = \sum_{n=-\infty}^{\infty} \left\{ \frac{2L_{st}R_s}{N_m} B_{gn} \int_{-\theta_s/2}^{\theta_s/2} K_{st}(\theta) e^{jn\theta} d\theta \right\} e^{jn\alpha} \tag{7.15}$$

where the expression inside the brackets is the Fourier series coefficients of the tooth flux. As it stands, computation of the Fourier series coefficients of the tooth flux requires computation of the given integral for every harmonic index n .

Elimination of this integral is possible by determining the Fourier series description of the slot correction factor (7.10) or (7.11), which is easily accomplished using the FFT approach described in Appendix A. Since the slot correction factor $K_{st}(\theta)$ is not periodic with respect to electrical measure, but rather with respect to the slot pitch, the integral in (7.15) must be rewritten in terms of an angular measure associated with the slot pitch. That is, a change of variable is required so that the limits on the integral are $-\pi$ and π respectively.

There are N_s slots and teeth. Therefore, there are N_s slot pitch periods per mechanical revolution and the relationship between slot measure and mechanical measure is

$$\theta_{sl} = N_s \theta_m \quad (7.16)$$

where θ_{sl} is angle in slot measure. Combining this with the relationship between electrical measure and mechanical measure $(2/N_m)\theta_e = \theta_m$ gives the desired relationship between electrical measure and slot measure as

$$\theta_{sl} = \frac{2N_s}{N_m} \theta_e \quad (7.17)$$

Using this relationship to change variables in the integral in (7.15) and writing the slot correction factor as the Fourier series

$$K_{sl}(\theta) = \sum_{m=-\infty}^{\infty} K_{slm} e^{jm\theta} \quad (7.18)$$

where θ is in slot measure, the integral in (7.15) simplifies to

$$\int_{-\theta_s/2}^{\theta_s/2} K_{sl}(\theta) e^{jn\theta} d\theta = \frac{\pi N_m}{N_s} \sum_{m=-\infty}^{\infty} K_{slm} \operatorname{sinc} \left[\left(m + n \frac{N_m}{2N_s} \right) \pi \right] \quad (7.19)$$

where $\operatorname{sinc}(x) = \sin(x)/x$. This expression allows (7.15) to be rewritten as

$$\phi_t(\theta) = \sum_{n=-\infty}^{\infty} \phi_{tn} e^{jn\theta} \quad (7.20)$$

where $\theta = \alpha$ is angular position in electrical measure and the Fourier series coefficients are

$$\phi_{tn} = B_{gn} \frac{2\pi R_s}{N_s} \sum_{m=-\infty}^{\infty} K_{slm} \operatorname{sinc} \left[\left(m + n \frac{N_m}{2N_s} \right) \pi \right] \quad (7.21)$$

These last two equations describe the tooth flux as a function of electrical measure. If these equations describe the tooth flux in the first tooth, then the tooth flux in the other teeth have the same shape but are delayed by the angular electrical distance between the teeth. For example, the tooth flux in the second tooth is $\phi_{t2}(\theta) = \phi_t(\theta - \theta_s)$ where $\theta_s = (N_m/N_s)\pi$ is the angular slot pitch in radE. Generalizing this relationship gives the tooth flux in the k th tooth

$$\phi_{tk}(\theta) = \phi_t(\theta - (k-1)\theta_s) \quad \text{for } k = 1, 2, \dots, N_s \quad (7.22)$$

If one assumes that the tooth flux spreads out uniformly across the tooth body in the region past the shoe area, the tooth body flux density is given simply as

$$B_t(\theta) = \frac{\phi_t(\theta)}{K_{st}L_{st}w_{tb}} = \sum_{n=-\infty}^{\infty} B_{tn}e^{jn\theta} \quad (7.23)$$

where

$$B_{tn} = \frac{\phi_{tn}}{K_{st}L_{st}w_{tb}} \quad (7.24)$$

in which K_{st} is the lamination stacking factor, L_{st} is the axial motor length, and w_{tb} is the tooth body width as shown in Fig. 7-5.

A typical tooth flux density distribution versus rotor position based on the above derivation is shown in Fig. 7-6. When the North pole of a magnet is centered over the tooth as it is at $\theta=0$ and $\theta=2\pi$, the flux density has maximum positive amplitude. Similarly, when the tooth is centered over a South pole at $\theta=\pi$, the flux density has maximum negative amplitude. In between these extremes, the tooth flux density varies in response to the net flux entering the tooth. For example, when the tooth is centered between a North and South pole, the tooth flux density is zero. The tooth flux and flux density inherit their zero average and halfwave symmetry properties from the air gap flux density distribution.

7.4 Stator Yoke Flux

Given the description of the flux in each tooth (7.22), the stator yoke fluxes can be determined. In this case, the tooth fluxes are known and are modeled as flux sources as shown in the partial magnetic circuit in Fig. 7-7. The stator yoke segments are constant reluctances whose fluxes are labeled with subscripts denoting the two teeth connected to each yoke segment. The MMF at each tooth and yoke segment connection relative to the center node is labeled according to tooth number as F_k , where k is the tooth number.

Setting the sum of fluxes leaving each tooth and yoke segment connection to zero, gives the N_s equations in N_s unknowns